Effect of Holes Arrangement on Effusion Cooling Performance

Dr. Muwafag Sh. Alwan
Electromechanical Engineering Department, University of Technology/ Baghdad
Dr. Reyadh Ch. Al-Zachary
Institute of Technology, Foundation of Technical Education / Baghdad
Email: reyadhc@yahoo.com

Received on: 12/8/2013 & Accepted on:9/1/2014

ABSTRACT

The present work concentrates on the experimental investigation of effusion cooling performance for different whole pitch ratios. The film cooling effectiveness and local heat transfer coefficient for difference jet holes arrangement have been investigated on a flat plate at three blowing ratios (0.5,1.0 and 1.5) at Reynolds number based upon hole diameter and hot main stream velocity is (6000). The investigations were done by using a single test transient IR the rmography technique. Three models of staggered holes arrangement are investigated. Each model is provided with seven rows of holes. The holes diameter (D) is 4mm, the longitudinal distance (X) are 8D, 10D and 12D respectively, and the span wise distance(S) between two neighboring holes are 7D.The attitude of the holes is fixed at inclination angle ($\theta = 30^{\circ}$). The experimental investigation shows that the thermal performance decreases as the pitch ratio (X/D) increases for all blowing ratios, and the film cooling effectiveness decreases as the blowing ratio increases for all the three models.

تأثير تنظيم الفتحات على أداء تبريد الانتشار

الخلاصة:

لقد تم التركيز في هذا البحث على أختبارات عملية لدراسة أداء تبريد الانتشار لنسب خطوة الفتحات. ولحساب فعالية غشاء التبريد ومعامل أنتقال الحرارة , تم اجراء تجارب عملية لفتحات نفث مختلفة التنظيمات على صفيحة مستوية لثلاث نسب نفخ (0.5,1.0 and 1.5)وكان عدد رينولدز المبني على اساس سرعة التيار الحار وقطر الفتحه هو (6000) بأستخدام تقنية الصورة الحرارية تحت الحمراء (IR)بالية الفحص الأنتقالي الواحد. لقد تم فحص ثلاث نماذج من الفتحات المتعرجة (stagger) الترتيب, وكل نموذج مزود بسبعة صفوف من الفتحات الدائرية. تم تثبيت قطر الفتحات (D)بمقدار (4 mm) والمسافة الطولية بين صف وأخر (X)بالمسافات (8D,10D, and 12D) على التوالي بينما تم تثبيت المسافة بين الفتحات المتجاورة (S)في الصف الواحد بمقدار 7D, وكذلك تم تثبيت زاوية ميل الفتحات بمقدار (30^{o}).

اظهرت النتائج العملية أن أداء التبريد يقل بزيادة نسبة المسافة الطولية لجميع نسب النفخ المدروسة,كما أظهرت النتائجأن فعالية غشاء التبريد تقل مع زيادة نسب النفخ للنماذج الثلاث المدروسة.

NOMENCLATURES

D	whole diameter	m
h	Heat transfer coefficient with film cooling	W/m2 •K
h_o	Heat transfer coefficient without film cooling	W/m2 •K
k	Thermal conductivity	W/m2 •K
S	Span wise hole spacing	m
t	time	s
T	Temperature	○C
T_c	Coolant temperature	○C
T_i	Initial temperature	○C
T_m	Hot mainstream temperature	○C
T_w	Wall temperature	○C
U_c	Coolant velocity	m/s
U_m	Hot mainstream velocity	m/s
η	Film cooling effectiveness	-
η_{av}	Average film cooling effectiveness	-
η_{sa}	Stream wise Average film cooling effectiveness	-
ρ	Density of air	kg/m3
ρ_c	Density of coolant air	kg/m3
ρ_m	Density of hot mainstream	kg/m3
θ	Inclination angle	Degree

INTRODUCTION

Thermal efficiency and power output of a gas turbine can be improved by means of higher turbine inlet temperature. Most of the modern gas turbine are now operating with turbine inlet temperature in the range of 1800 K to 2000 K, which near the melting point of the alloys used in the turbine components; to increase the lifespan and to prevent these components from failing the walls of these components must be protected against the high surrounding temperature,methods such as coating applications, film cooling (also referred to as effusion cooling) become necessary.

Film cooling intended to protect the turbine components surface from having a direct contact with the hot gases by the injection of the coolant fluid through the surface into the external boundary layer. The injected cold air will form a buffer layer of relatively cool air between the surface and the hot gases contained within the turbine flow path.

Effusion (or transpiration) cooling, which contains an array of closely spaced discrete film cooling holes, is widely used to cool and insulate the component metal from the hot mainstream flow. The cooling effectiveness of an effusion cooling plate depends on several parameters, such as whole spacing, angle, diameter, etc.

Review on turbine cooling technology developments has been well described by Han et al. [1], Bunker [2] covering of all the available technologies on film cooling. Han and Rallabandi [3**]** stated that the pressure sensitive paint technique proved very high resolution contours of film cooling effectiveness, without being subjected to the conduction error in high thermal gradient regions near the hole. Andrews et al. [4] investigated (90 deg.) cooling hole for a number of different arrays and found that there was a significant improvement in the overall cooling effectiveness for a larger hole relative to a smaller hole. Andrews et al. [5] also compared normal (90 deg.) and

inclined film holes (30 deg. and 150 deg.) for an array of effusion holes and found that cooling effectiveness improved with inclined holes. The counter flow holes (150 deg.) resulted in reverse flow and good cooling performance at low coolant flows but not at high coolant flows.

Martiny et al. [6] used a very low injection angle of (17 deg.) for an effusion, film cooling plate in which they measured adiabatic effectiveness levels for a range of blowing ratios. Their results indicated significantly different flow patterns depending on the cooling jet blowing ratio. It is important to recognize that their study used only four rows of cooling holes and as will be shown in this paper, this small number of rows did not allows for a fully developed condition to occur.

Gustafsson and Johansson [7] investigated the temperature ratios and velocity ratios between hot gas and coolant, and different injection hole spacing, inclination angle, and thermal conductivity of the test plate.

Ekkad et al. [8] obtained both film cooling effectiveness and heat transfer coefficient from a single test by means of the transient infrared thermography technique. The advantage of IR technique was exhibited adequately in these previous research efforts. In terms of the wider temperature range handled than the liquid crystal technique and more detailed 2D temperature field information with better accuracy. It is seen that these research with successful employed of the IR technique enriched higher quality data in the literature, but the effect of the deflection angle of the injection holes was not attempted.

Dhungel et al. [9] obtained simultaneously detailed heat transfer coefficient and film effectiveness measurements using a single test transient IR thermography technique for a row of cylindrical film cooling holes, shaped holes. A number of anti-vortex film cooling designs that incorporate side holes. They found that the presence of anti-vortex holes mitigates the effect of the pair of anti-vortices.

Diaand Lin [10] investigated numerically three film cooling configurations, (cylindrical hole, and shaped whole, crescent hole). All holes were inclined at 35° on a flat plate. All simulations are conducted at blowing ratio of 0.6 and 1.25, length to diameter ratio of 4 and pitch-to-diameter ratio of 3. They use (RANS) equations, the energy equation, and two-layer $(k-\epsilon)$ turbulence models. For the numerical investigation the commercial CFD software FLUENT with standard $(k-\epsilon)$ turbulent models is applied. They found that the crescent hole exhibits the highest film cooling effectiveness among the three configurations both in spanwise and streamwise especially downstream of the interaction of the two holes.

Numerical prediction of Alwan [11] shows that the flow field structure of injected holes present vortices, such as counter pair kidney vortex and horseshoe vortex have major effects on cooling performance, in which the strength of the kidney vortex decreases and the horseshow vortex is lifting up, leading to an improvement in the coolant performance. Therefore, numerical model is suitable to design holes arrangement futures of film cooling system by introducing oriented holes row over single jet holes row.

At the present work, experimental investigations were done to evaluate the film cooling performance for different hole pitch ratio and different blowing ratio in order to determine the heat transfer coefficient and the film cooling effectiveness on a flat plate by using a single test transient IR thermograph technique.

EXPERIMENTAL FACILITIES

Low speed open duct jet test rigwas used at the present investigation. A schematic diagram of the test rigare shown in figure1. The mainstream air supply is the ambient air drawn by a centrifugal backward blade blower. The blower is driven by 2.5 kW motor running with 2800 rpm. Manual open gate is used to control the air speed in the tunnel test section. The blower exit area having rectangular shape with dimensions of (6.3x13.1) cm. The blower is supplied with bend having the same dimensions of the blower exist and then connected to a diffuser having rectangular cross-section area of inlet and outlet dimensions as (6.3x13.1) cm and (35x50) cm respectively and length of (82) cm. Air flow diffuses over a splitter plates into a constant area rectangular settling chamber of cross-section area (35x50) cm and length of 70 cm. The settling chamber contains a series of three electrical heaters each of 4 kW power and four grid screen. This ensures adequate mixing of hot air and uniform temperature distribution throughout the test section. Then the hot air routed through a convergent- divergent contraction having a rectangular cross-section area from (35x50) cm to (5x10) cm and length of 70 cm. In order to allow the air to reach the desired temperature, the air is initially routed out away from the test section by using a by-bass gate passage. The temperature of the air is continuously monitored at the exit of the gate and when the desired temperature is reached, the gate is fully opened manually and air flow passes into a test section through a rectangular duct area. To minimize heat losses to the surrounding the settling chamber and the test section duct are insulated completely. The operating velocity of the hot air in the test section is controlled to run from 20 to 40m/s through the experimental program. The test section has 50mm width and 100mm height. The bottom plate of the test section is made of (234x123) mm Plexiglas of 10mm thickness.

A centrifugal air blower of blowing capacity of (22.17) m^3/min was used to supply the coolant air to the plenum. The plenum was located below the test plate. The coolant air enters a plenum then ejected through holes into the test section. The coolant air pressure measured at the inlet of the test section. Digital thermometers were used to measure the mainstream and coolant air temperature. Pre-testing showed that all holes had the same flow rate and temperature conditions.

The coolant air injected from the holes is mixed with the hot mainstream in the test section. The test section has 5 cm width, 10 cm height and 23.4 cm length. The bottom wall of the test section work as a test model, three models with different hole pitch ratio are prepared, each model made of (234x100) mm Plexiglas plate of 10mm thickness. The bottom model plate can be removed easily to be replaced by another model at each test. Each model is provided with seven rows of holes, these models are arranged with staggered row holes. The holes diameter is 4mm, the longitudinal distance (X/D) are 8D, 10D and 12D respectively, and the span distance between two neighboring holes (S/D) are 7D as shown in Figure (2). The attitude of the holes is fixed at inclination angle ($\theta = 30^{\circ}$), where the inclination angle (θ) is defined as the angle between the centerline of the hole and the surface of the test wall. Data is taken for only three middle rows of holes to reduce the effects of the side wall.

SURFACE TEMPERATURE MEASUREMENT

The surface temperature of test model was measured using an infrared thermographs technique. IR thermograph infrared camera type Fluke Ti32 was used in the present investigation. This camera is able to precisely record the temperature variations. The IR system is greatly affected by both background temperature and

local emissivity. The test surface is sprayed with mat black color to increase the emissivity like a perfect black body. The temperature measurement taken is not accurately recorded unless the IR system is calibrated.

The system was calibrated by measuring the temperature of the test surface using thermocouple type K and the reading of IR camera. The test surface is heated by mainstream hot air. The measured temperatures obtained by both ways are recorded and stored during the heating process until achieving a steady state condition. Due to the emissivity of the test surface, the temperature obtained by IR camera is different from the temperature obtained by the thermocouple. Therefore, the IR camera reading is adjusted until both temperature readings are matched.

The IR images taken for the test surfaces at each test are stored in the SD memory of IR camera. These images are transferred from SD memory to PC memory. Then the middle region of the test surface area is then selected to eliminate the effect of the test section wall with using camera software, Smart View Software Program. IR images, which exhibit the temperatures distribution as colors code, is converted to corresponding temperature digit values by using Smart View Software and then saved as output datain Excel sheet.

FILM COOLING EFFECTIVENESS AND HEAT TRANSFER COEFFICIENT ESTIMATION

The heat transfer model associated with film cooling is a so-called three temperature problem. Typically, the heat flux from flow to surface without film cooling is expressed as:

$$q_o = h_o(T_m - T_w) \quad \dots (1)$$

In this case, T_m-$T_w$is the driving potential for heat transfer; thus it is called a two-temperature problem. While film cooling flow is injected on the surface, the flow downstream of a film cooling hole is mixture of mainstream and the coolant. The heat flux to surface can be described as:

$$q = h\,(T_f - T_w) \quad \dots (2)$$

Balancing thermal energy in the surface of the test plate and conducted in the X-direction yields the following equations:

$$\frac{\partial^2 T}{\partial x^2} = \frac{1}{\propto}\frac{dr}{dt} \quad \dots (3)$$

Two boundary conditions are needed. Initial condition to solve this partial differential equation is such as: at t=0 , $T=T_i$The first boundary condition is at the wall surface, at x=0 and $t \geq 0$.

$$-k\frac{\partial T}{\partial x} = h(T_m - T(0,t))$$

The main assumption applied to analyze the transient conduction is the semi-infinite approximation. The semi-infinite solid assumptions give an additional boundary condition, at $x = \infty$, $T=T_i$ and $t \geq 0$. At present investigation the

test surface is modeled as a semi-infinite solid medium imposed by a sudden transient heating. The entire solid medium is initially at a uniform temperature before the transient test. During the transient heating test, each point on the surface responded to temperature difference per time difference due to different heat transfer coefficient. The test surface is modeled as under going 1-D transient conduction with convective boundary conditions at the wall. Applying the prescribed boundary conditions and initial conditions to the problem and solving for the wall temperature response relation to time at the wall. Therefore, the solution of one-dimensional transient conduction equation is done according to Incropera and Dewitt [12].

By combining film cooling effectiveness and heat transfer coefficient, the ratio of heat flux q to film-protected surface to that of of the corresponding baseline value without film cooling q_o can be expressed as:

$$\frac{q''}{q''_o} = \frac{h}{h_o}\left(1 - \frac{\eta}{\emptyset}\right) \quad \ldots (4)$$

Where the overall cooling effectiveness given by $Ø= (T_w-T_m)/ (T_c-T_m)$, the typical value Ø in actual engines range from 0.5 to 0.7 (Yu et al. [ ]) in the main body section. The average value of 0.6 is used in the calculation of the present studies.

In order to obtain the cooling variation trend in the streamwise direction, the spanwise averaged cooling effectiveness at each streamwise location (X/D) is calculated by $\eta_{sa} = \sum \eta_i /N$, where N is the number of data points in the spanwise direction.

The IR images for models surface at each investigated test was captured and stored by a thermal camera. These images are transferred to PC. Smart View Software program supplied with Camera can be used to limit the selected area to avoid the effect of the test section walls. The IR images converted to corresponding temperature digital values and then saved as data in Excel sheet.

MATLAB Software programs are prepared using a semi-infinite solid assumption to introduce the film cooling effectiveness and heat transfer coefficient contours. Equations, (4), (5), (6), and (7) may be solved using MATLAB Software, Smart View Software, and Excel Software.

The measurement uncertainty was determined by using the methodology described by Holman and Bhattacharyya [13].Error estimates for each variable are as follows: wall temperature $\Delta T_w = \pm 2$ ºC, initial temperature $\Delta T_i = \pm 2$ ºC, mainstream temperature $\Delta T_m = \pm 0.2$ ºC, and coolant temperature $\Delta T_c = \pm 0.2$ ºC.The camera frame rate is 60 Hz resulting in a time error $\Delta t = \pm 0.125$ sec. and the test surface properties (α and k) uncertainty are taken from tabulated values, as a custom, 3%relative uncertainty is assumed for both variables. The resulting average uncertainty for heat transfer coefficient and film effectiveness is ±8.2% and ±11.0%, respectively.

RESULTS AND DISCUSSIONS

Figures (3 to 5) show the effect of hole pitch ratios (X/D) on the temperature distribution for different blowing ratios (BR= 0.5, 1.0, and 1.5). Comparison between model 1, model 2 and model 3 showed that the model 1 gave high protection than the model 2 also model 2 give high protection than model 3, for the three blowing ratios. Also Figures (3 to 5) show that the coolant temperature distribution decreases as the blowing ratio increases for all the three models. The reason is that for a low momentum ratio of about (i. e. BR=0.5), the mainstream flow close to the test

surface, the jet streamlines seems to go towards the surface and the mainstream flow depart upward, therefore the mainstream push the jet towards the surface, and the interaction forms a low temperature film layer near the wall and give high protection effect, while for a high momentum ratio (i. e. BR=1.5), coolant jets have enough momentum to penetrate in to the cross mainstream. These results agree well with the results obtained by sun et al. [14].

Figure (6) presents the stream wise averaged film effectiveness (η_{sa}). (η_{sa}) is calculated as the average values taken from the local reading of 197 pixels in stream wise direction in eighteen streamlines location downstream from the hole exist. Figures (6.a, 6.b and 6.c) show that the model 1 gave high values of (η_{sa}) as compared to the two other models (model 2 and model 3). The overall average film cooling effectiveness (η_{av}) was calculated from the values of local film cooling effectiveness (η) for all the entire pixels values.

Figure (7) shows the effect of blowing ratio on (η_{av}) for the three models. This figure shows clearly that the values of (η_{av}) for the model 1 are higher than the other two models. It appears also that the values of (η_{av}) decreases as the blowing ratio increases for all the three models.

As a matter of fact, the enhancement of the blade surface protection is done by keeping the local heat transfer coefficient (h) as low as possible. The local heat transfer coefficients are calculated from the data of two IR images taken in successive times as described above. The average of the local heat transfer coefficient ratios (h / h_o), in which (h and h_o) represent the heat transfer coefficient on the plate surface with and without film cooling respectively are presented in Figure (8). The values of the average heat transfer coefficient ratio for the model 1 are higher than that the two other models for all blowing ratios and (h/ho) is increased with increasing the blowing ratio. The increment of (h/ho) is due to that the jet injection produces high turbulence level inside the mixing region.

In the practical application, turbine designers are concerned with the reduction of heat load to the film protected surface. The heat load can be presented by combining film cooling effectiveness (η) and the heat transfer coefficient ratio (h/h_o), according to equation (7), therefore the ratio (q/q_o) can be calculated. (q/q_o) represent the reduction in heat flux at the tested surface with the presence of coolant air. If the values of these ratios are less than 1, then the film coolant is beneficial according to Lu et al. [15],while if the values are greater than 1, therefore effect of the film coolant is poor.

Figure (9) shows the effect of the blowing ratio on the overall heat flux ratios (q/q_o). It is clear that from this Figure the model 1 provides significant reduction of heat flux at all tested BR than that of the other models.

CONCLUSIONS

The present work has reached to the following conclusions:

1- The thermal performance decreases as the pitch ratio (X/D) increases for all blowing ratios.
2- The film cooling effectiveness decreases as the blowing ratio increases for all the three models.
3- The values of the average heat transfer coefficient ratio (h/ho) for the model 1 are higher than that the two other models for all blowing ratios and (h/ho) is increased with increasing the blowing ratio.

4- The model 1 provides significant reduction of heat flux at all tested BR than that of the other models.

REFERENCES

[1].Han, J.C., Dutta, S. andEkkad, S., 2000,"Gas Turbine Heat Transfer and Cooling Technology", Taylor and Francis, New York, pp. 129-136.

[2].Bunker, R.S.,2009, "Film Cooling: Breaking the Limits of Diffusion Shaped Holes", Proceeding of International Symposium on Heat Transfer in Gas Turbine, Antalya, Turkey.

[3].Han, J.C. and Rallabandi, A. P.,2010, "Turbine Blade Film Cooling Using PSP Technique", Frontiers in Heat and Mass Transfer, Texas, 77843-3123, USA.

[4].Andrews, G.E., Khalifa, I.M., Asere, A.A., and Bazdidi-Tehrani, F. 1995," Full Coverage Discrete Hole Film Cooling: The Influence of Hole Size", ASME 85-GT-47.

[5].Andrews, G.E., Asere, A.A., Gupta, M.L., and Mkpadi, M.C., 1985," Full Coverage Effusion Film Cooling with Inclined Multihole Walls with Different Hole Arrangements", ASME GT2003-38881.

[6].Martiny, M., Schulz, A., and Witting, S. 1995," Full coverage Film Cooling Investigations Adiabatic Wall Temperature and Flow Visualization", ASME 95-WA/HT-4.

[7].Gustafson, K.M., and Johansson, T., 2001, " An experimental Study of Surface Temperature Distribution on Effusion- Cooled Plates", Journal of Engineering for Gas Turbines and Power Transactions of the ASME 123(2001) 308-316.

[8].Ekkad, S.V., Shichman, O., and Bunker, R.S., 2004, "Transient Infrared Thermography Method for Simultaneous Film Cooling Effectiveness and Heat Transfer Coefficient Measurement from a Single Test", Journal of Turbo machinery Transactions of the ASME 126(2004) 597-603.

[9].Dhungel, A., Phillips, A., Ekkad, S.V., and Heidmann, J.D., 2007, "Experimental Investigation of a Novel Anti-Vortex Film Cooling Hole Design", ASME IGTI Turbo Expo, Montreal, Paper GT 2007-27419.

[10].Dia, P. and Lin, F., 2011, "Numerical study on film cooling effectiveness from shaped and crescent holes", Heat Mass Transfer, Vol. 47, PP. 147-154.

[11].Alwan, M.Sh., 2012," Experimental and Numerical Investigation of Film Cooling Thermal Performance for Staggered Rows of Circular Jet", PhD Thesis, Mechanical Engineering Department, University of Technology.

[12].Incropera, F. P., and DeWitt, D. P., 2002, "Fundamentals of heat and mass transfer", Fifth Edition, New York, John Wiley & Sons.

[13].Holman, J.P. and Bhattacharyya, S., "Heat Transfer", Ninth Edition, New Delhi, McGraw-Hill, 2008.

[14].Sun, W., Chao, J.H., Chen, Y.W., and Miao, J.M., 2009, "Numerical study on the Effusion Cooling Performance over the Walls of an Annular Burner", Seventh International Conference on CFD in the Minerals and Industries CSIRO, Melbourne, Australia.

[15].Lu, Y., Dhungel, A., Ekkad, S.V., and Bunker, R.S., 2007, "Film cooling measurements for cratered cylindrical inclined holes", ASME Paper GT 2007-27386.

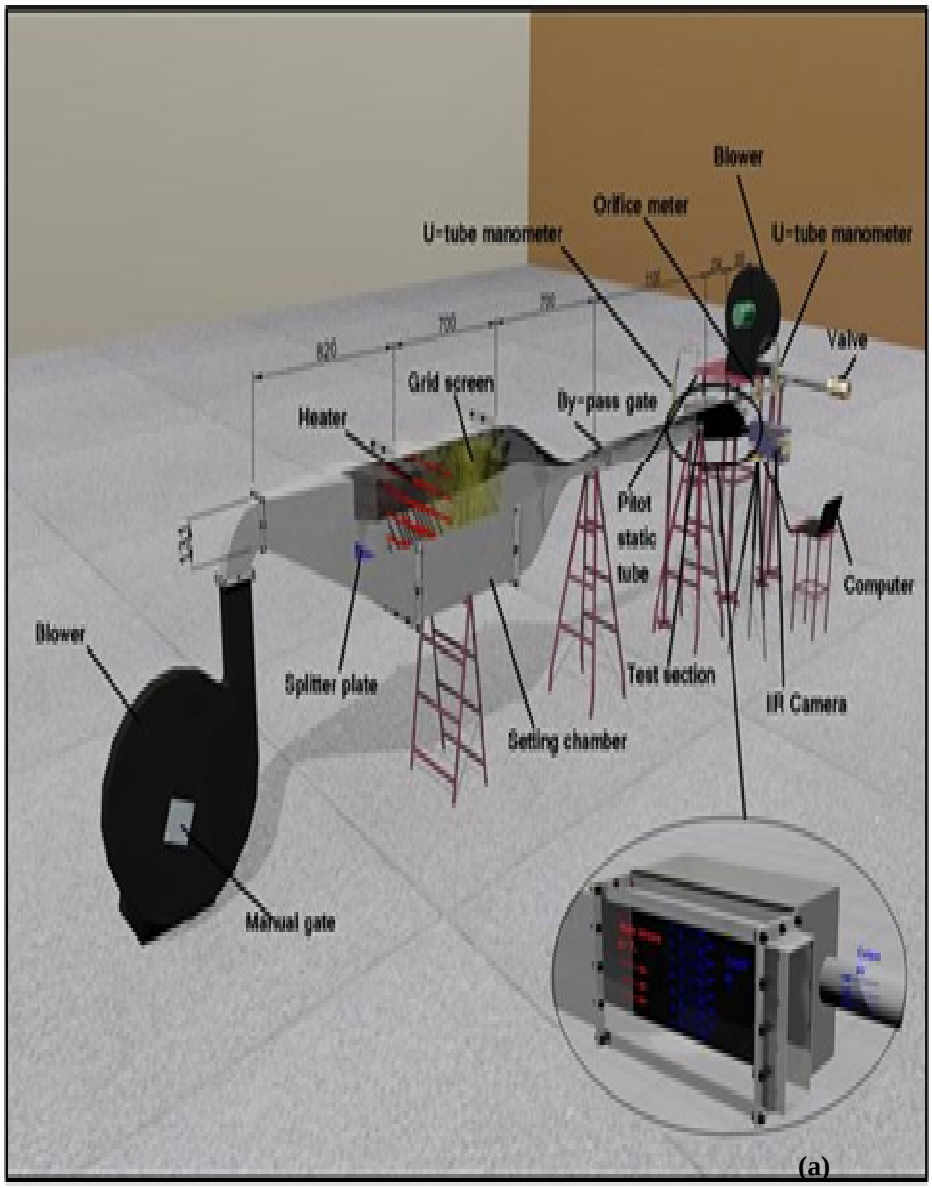

Figure (1) Schematic of the test rig.

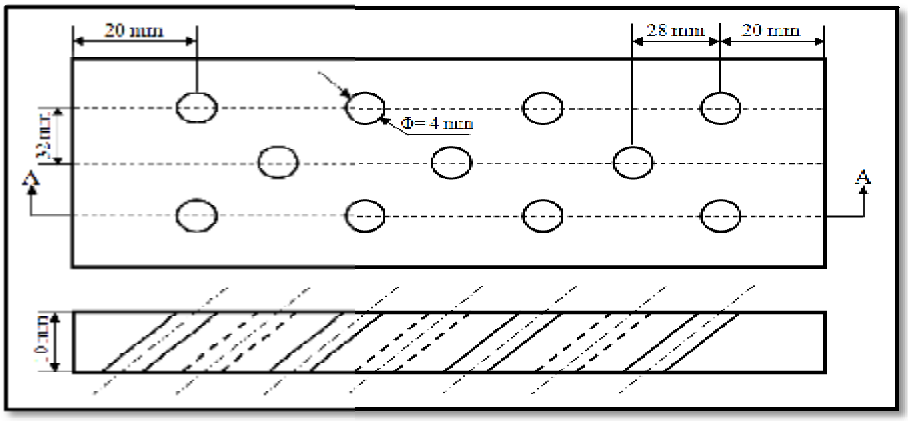

(a)

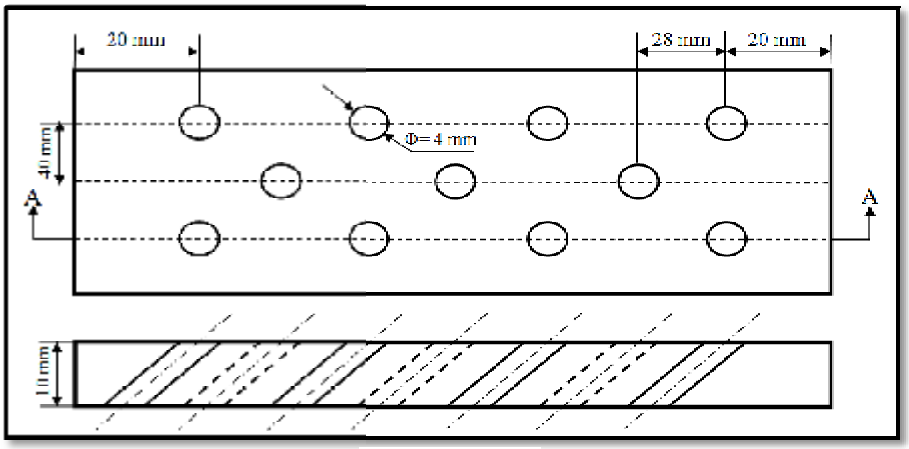

(b)

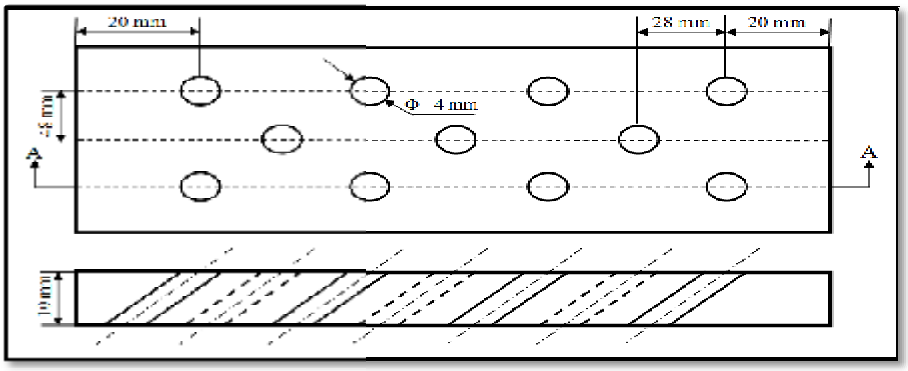

(c)

Figure (2) Details of three test models :(a) X/D=8 & S/D=7, (b) X/D=10& S/D=7, and (c) X/D=12& S/D=7.

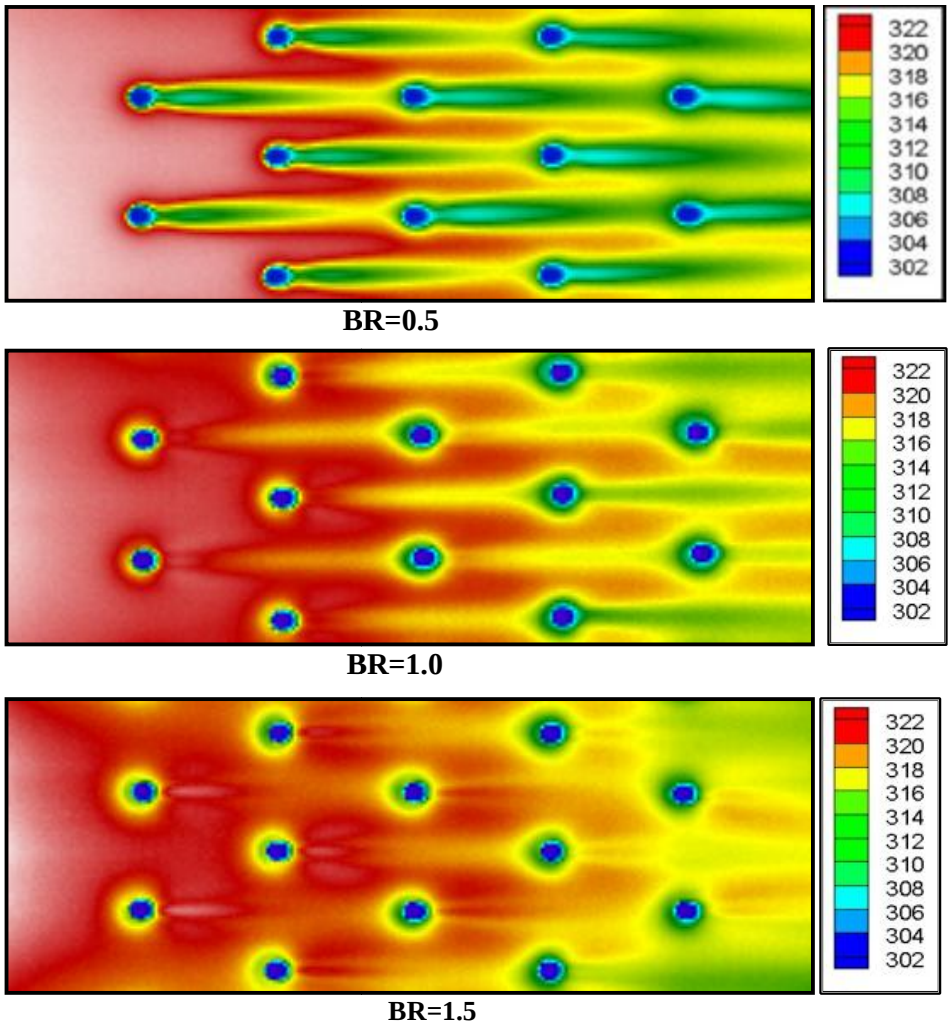

Figure (3) Contours of temperature distribution for model 1 (X/D=8 & S/D=7) at different blowing.

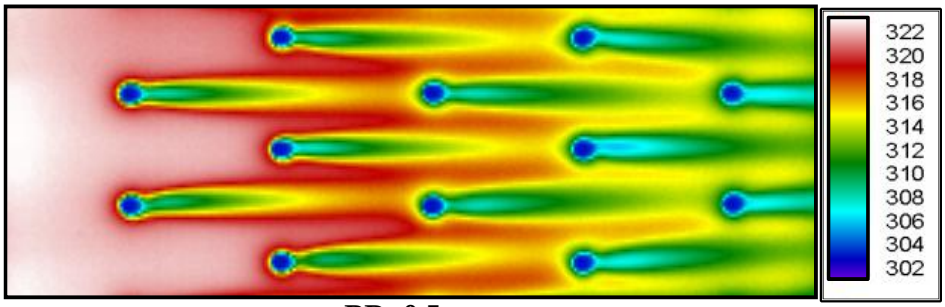

BR=0.5

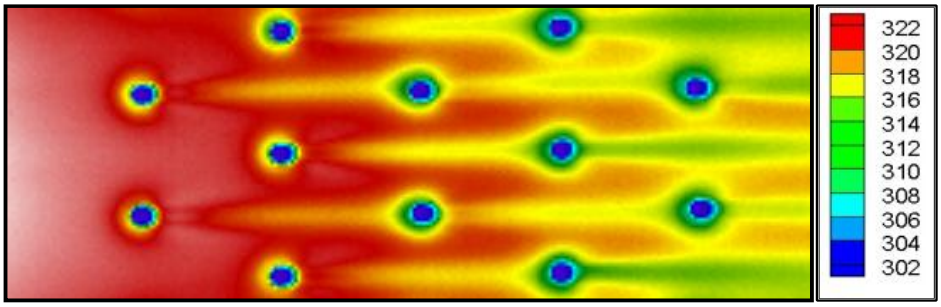

BR=1.0

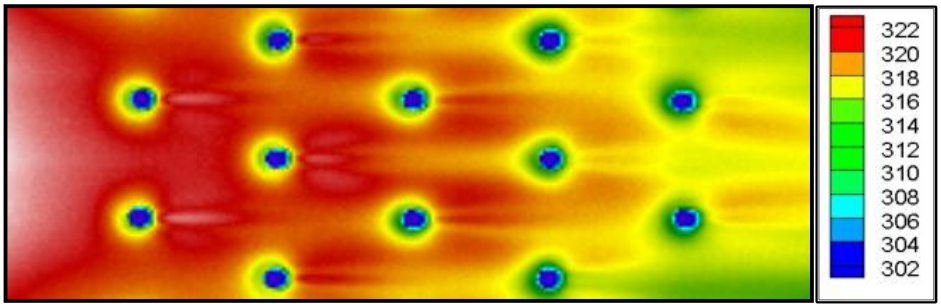

BR=1.5

Figure (4) Contours of temperature distribution for model 2 (X/D=10 & S/D=7) at different blowing.

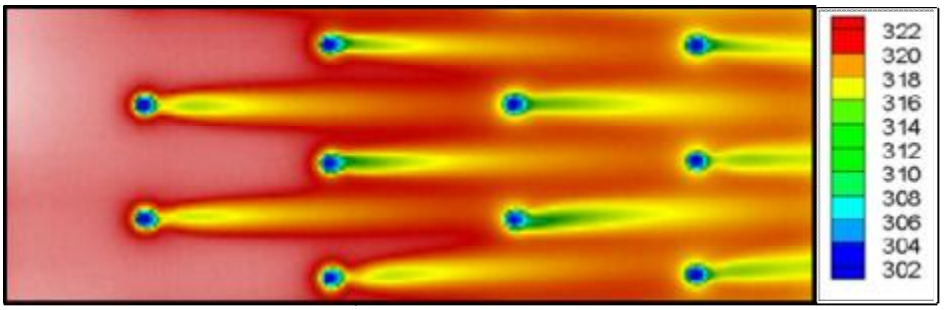

BR=0.5

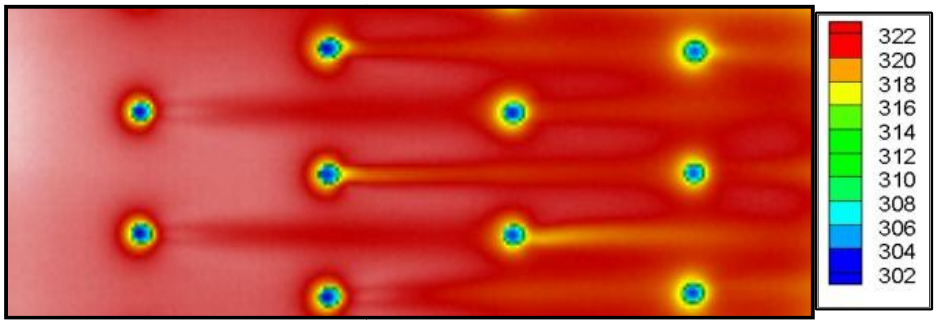

BR=1.0

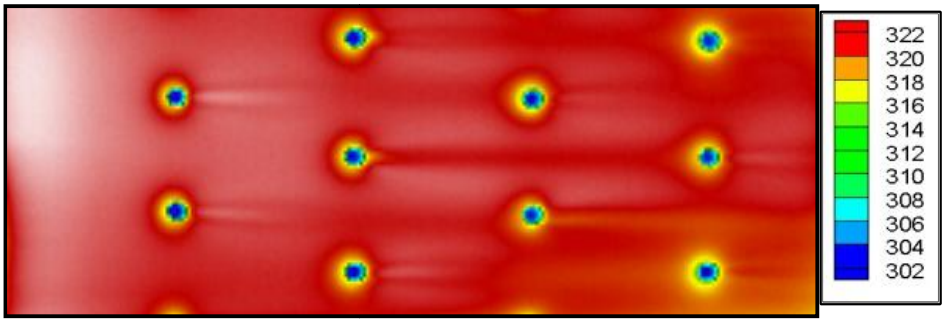

BR=1.5

Figure (5) Contours of temperature distribution for model 3 (X/D=12 & S/D=7) at different blowing.

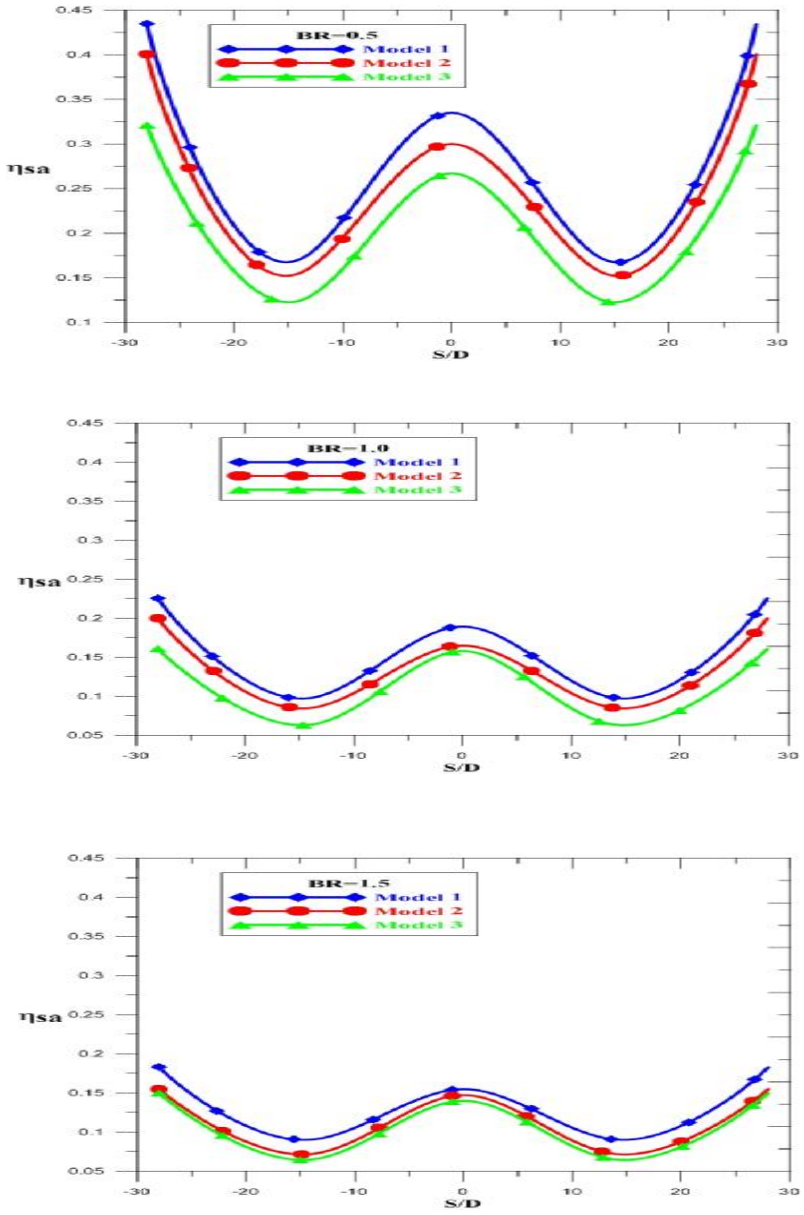

Figure (6) Effect of pitch spacing (X/D) on span wise averaged film cooling effectiveness at: (a) BR=0.5, (b) BR=1.0, (c) BR=1.5 for models (1, 2 and 3).

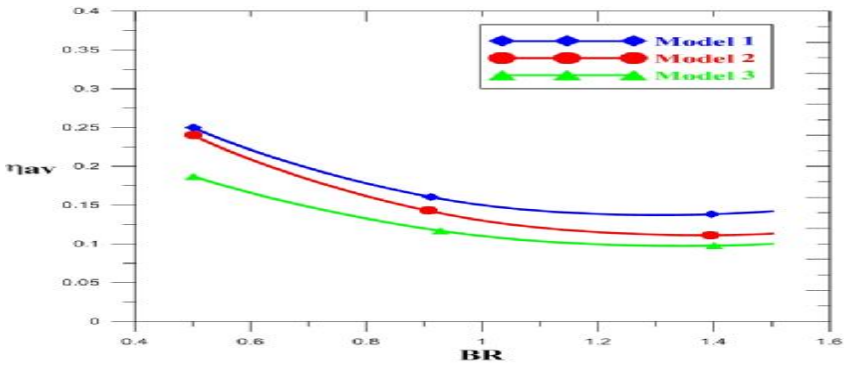

Figure (7) Effect of blowing ratio on averaged film cooling Effectiveness for models (1, 2 and 3).

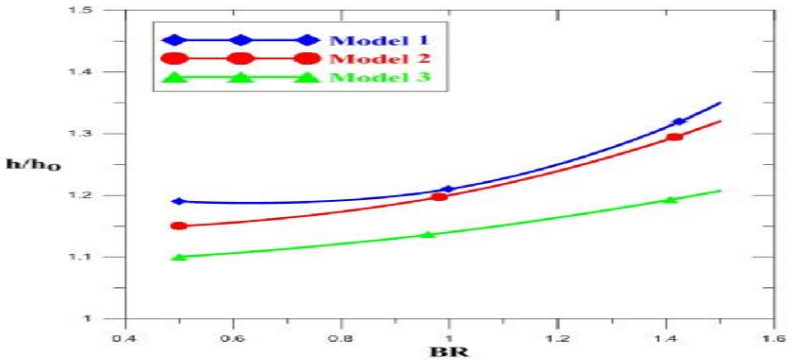

Figure (8) Effect of blowing ratio on averaged heat transfer coefficient for models (1, 2 and 3).

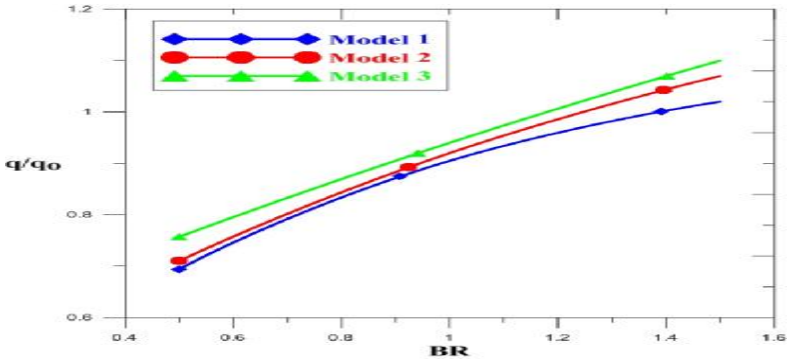

Figure (9) Effect of blowing ratio on overall heat flux ratio for models (1, 2 and 3).